Mott transitions in three-component Falicov-Kimball model

Duong-Bo Nguyen and Minh-Tien Tran
Institute of Physics, Vietnam Academy of Science and Technology, 10 Dao Tan, Hanoi, Vietnam
(Received 5 November 2012; published 24 January 2013)

Metal-insulator transitions are studied within a three-component Falicov-Kimball model, which mimics a mixture of one-component and two-component fermionic particles with local repulsive interactions in optical lattices. Within the model, the two-component fermionic particles are able to hop in the lattice, while the one-component fermionic particles are localized. The model is studied by using the dynamical mean-field theory with exact diagonalization. Its homogeneous solutions establish Mott transitions for both commensurate and incommensurate fillings between one-third and two-thirds. At commensurate one-third and two-thirds fillings, the Mott transition occurs for any density of hopping particles, while at incommensurate fillings, the Mott transition can occur only for density one-half of hopping particles. At half-filling, depending on the repulsive interactions, the reentrant effect of the Mott insulator is observed. As increasing local interaction of hopping particles, the first insulator-metal transition is continuous, whereas the second metal-insulator transition is discontinuous. The second metal-insulator transition crosses a finite region where both metallic and insulating phase coexist. At third-filling, the Mott transition is established only for strong repulsive interactions. A phase separation occurs together with the phase transition.

DOI: 10.1103/PhysRevB.87.045125 PACS number(s): 71.27.+a, 71.30.+h, 71.10.Fd, 03.75.Ss

I. INTRODUCTION

Metal-insulator transition (MIT) is a long standing problem in condensed matter physics and has attracted a lot of attention. The Mott insulating state is established when conduction electrons become localized due to the suspension of the double occupation by electron correlations.[1] Most studies on the MIT focus on electron systems with local Coulomb interaction between the two spin states of electrons. The achievement of loading ultracold fermionic atoms in optical lattices has been providing a novel stage for studying the Mott transitions.[2] Indeed, the Mott insulating state was realized for ^{40}K fermionic atoms with two hyperfine states and repulsive interaction between them.[3,4] This MIT is similar to the one of electron systems. Moreover, ultracold fermionic atom mixtures can be extended to have both large hyperfine multiplet and different masses. A mixture of single-spin state ^{40}K immersed in two-component fermionic atoms ^{6}Li or a mixture of two-component state ^{171}Yb and six-component state ^{173}Yb were established.[5,6] Such achievements lead to a possibility of studying the Mott transitions in multicomponent correlation systems. Theoretically, the Mott transitions in three-component Hubbard models were studied.[7,8] Within the dynamical mean-field theory (DMFT), the Mott transition is observed at commensurate fillings when the local Coulomb interactions are isotropic.[7] When the anisotropy of the local Coulomb interactions is introduced, the Mott transition is also observed at incommensurate half-filling.[8] However, in these studies, all component particles have the same masses. The mixtures of ultracold atoms are often established with mass imbalance. The mass imbalance could affect the MIT. Indeed, the DMFT of the mass-imbalance mixtures shows that the light particles may be more affected by correlations than the heavy ones.[9]

In this paper, we study the Mott transitions in a three-component Falicov-Kimball model (FKM). This model can be viewed as a version of the three-component Hubbard model[7,8] with extreme mass imbalance. Within the model, one-component fermionic particles are extremely heavy and localized. They are immersed in an optical lattice, where two-component fermionic particles with light mass can hop. Local repulsive interactions between the component states of particles are taken into account. The three-component FKM can be realized by loading mixtures of two species of fermionic atoms into an optical lattice. One species is single-spin state heavy atoms and the other is two-component light atoms. Such ultracold atomic mixtures can be realized by mixtures of ^{40}K with ^{6}Li, or light ^{6}Li or ^{40}K with heavy fermionic isotopes of Sr or Yb. When the mixtures are loaded into an optical lattice, the heavy atoms usually have much lower tunneling rate than the light atoms. With sufficient lattice depth, the hopping rate of the heavy atoms can be ignored in comparison with the one of the light atoms.[10] Similar mixtures of two species of one-component fermionic atoms were also proposed for the realization of the spinless FKM.[11] The three-component FKM can be considered as a complement of the three-component Hubbard model, when a strong mass imbalance is realized. Traditionally, the FKM was introduced to describe the MIT in rare-earth and transition metal compounds.[12] The spinless version of the FKM has a rich phase diagram, and in particular, the homogeneous states establish a correlation-driven MIT. At low temperature, charge-density-wave states are established.[13] The FKM can be extended to have additional terms in order to study different physical phenomena.[14–16] Multicomponent extensions of the FKM were also considered.[17,18] However, in the multicomponent versions of the FKM, the multiplicity of electron spins is just a formal generation of the spinless case, and the Coulomb interactions between the conduction electrons are not taken into account. In this paper, the three-component FKM keeps all local Coulomb interactions between the component states. In contrast to the spinless case, there is very little knowledge of the physical properties of the multicomponent FKM.[19]

The three-component FKM can also be considered as a combination of the Hubbard model of the two-component

hopping particles and the spinless FKM of the one-component localized particles. At half-filling, the Hubbard model exhibits an MIT, which is driven by the Coulomb interaction.[20] The insulating state is naturally the Mott insulator,[1] where the double occupation is suspended by the Coulomb interaction. The MIT is discontinuous.[21,22] At half-filling, the spinless FKM also displays an MIT, although this MIT is continuous.[18] When the Coulomb interaction is large enough, it also prevents the hopping and localized particles to occupy at the same site. As a result, the insulating state is established. One may expect that the three-component FKM could exhibit a rich phase diagram of the MIT. Indeed, in the present paper, we find both continuous and discontinuous MIT. The MIT can occur not only at half-filling, but also at other fillings between one-third and two-thirds.

In the present paper, we study the three-component FKM by using the DMFT with exact diagonalization (ED). The DMFT has been widely and successfully used to study the strongly correlated electron systems.[23,24] It has been also extensively applied to study the FKM.[18,25] The previous studies of MIT in the three-component Hubbard model were also based on the DMFT.[7,8] The advantage of the DMFT is that it is exact in infinite dimensions and fully captures local time fluctuations. However, the DMFT loses nonlocal correlations of finite dimension systems. Within the DMFT, we find that like the three-component Hubbard model,[8] the three-component FKM exhibits the Mott transition at both commensurate and incommensurate fillings. However, in contrast to the three-component Hubbard model, the MIT can occur at any filling between one-third and two-thirds. We also find an inverse MIT, i.e., the transition from insulator to metal when particle correlations increase. The inverse MIT can occur only in the region of large repulsive interactions between localized and hopping particles. At half-filling, a reentrant effect of the Mott insulator is observed. With increasing Coulomb interactions, the system first stays in the insulator region, then it becomes metallic, and finally goes back to the insulating phase. The first transition is continuous, while the second one is discontinuous. At the second MIT, we observe a finite region where both metallic and insulating phases coexist, like the MIT in the single-band Hubbard model.[21,24] However, in contrast to the single-band Hubbard model, the MIT in the three-component FKM is due to a superposition of two Kondo resonances that are shifted from the Fermi level. At one-third and two-thirds fillings, the Mott transition is established only for strong repulsive interactions and a phase separation occurs together with the phase transition.

The present paper is organized as follows. In Sec. II, we present the three-component FKM and its DMFT. The general filling conditions for the MIT are presented Sec. III. In this section, we also study the MIT at half- and third-fillings in details. Finally, the conclusion is presented in Sec. IV.

II. THREE-COMPONENT FALICOV-KIMBALL MODEL AND ITS DYNAMICAL MEAN-FIELD THEORY

We consider a three-component FKM that describes a mixture of one-component heavy fermionic particles and two-component light fermionic particles loaded in an optical lattice. The heavy particles are localized, whereas the light particles can hop in the lattice. Its Hamiltonian reads

$$H = -t \sum_{\langle i,j\rangle,\sigma} c^{\dagger}_{i\sigma} c_{j\sigma} + U_{cc} \sum_{i} c^{\dagger}_{i\uparrow} c_{i\uparrow} c^{\dagger}_{i\downarrow} c_{i\downarrow} + E_f \sum_{i} f^{\dagger}_{i} f_i + U_{cf} \sum_{i\sigma} f^{\dagger}_{i} f_i c^{\dagger}_{i\sigma} c_{i\sigma}, \quad (1)$$

where $c^{\dagger}_{i\sigma}$ ($c_{i\sigma}$) is the creation (annihilation) operator for a fermionic particle with hyperfine multiplet (or spin) σ at site i. σ takes two values ± 1. t is the hopping parameter of the two-component fermionic particles, and we take into account only the hopping between nearest-neighbor sites. U_{cc} is the local Coulomb interaction between the two-component states of those particles. $f^{\dagger}_{i}$ (f_i) is the creation (annihilation) operator for a one-component (or spinless) fermionic particle at site i. U_{cf} is the local Coulomb interaction between the two-component particles and one-component particles. The one-component particle does not move, and its energy level is E_f. E_f can also be considered as the chemical potential of the localized particles and controls the filling of the localized particles $n_f = \sum_i \langle f^{\dagger}_{i} f_i \rangle / N$, where N is the number of lattice sites. A common chemical potential μ is introduced to control the total particle filling $n = \sum_{\sigma} n_{c\sigma} + n_f$, where $n_{c\sigma} = \sum_i \langle c^{\dagger}_{i\sigma} c_{i\sigma} \rangle / N$. The three-component FKM has two well-known limiting cases. When $U_{cf} = 0$ the two-component and one-component particles are completely decoupled. The Hamiltonian of the two-component particles is just the single-band Hubbard model.[20] Within the DMFT, the Mott insulating phase is established at half-filling and sufficient large local Coulomb interactions. The MIT is of first order.[21,24] When $U_{cc} = 0$, the model in Eq. (1) is equivalent to the spinless FKM.[12] Within the DMFT its homogeneous phase also displays a MIT.[18] However, the metallic phase breaks the Fermi liquid theory due to the pinning of the chemical potential at the localized particle level.[26] The MIT is continuous. The model in Eq. (1) can also viewed as a simplified version of the three-component Hubbard model[7,8] with strong mass imbalance, where the particles of one specified component are heavy and localized. The three-component FKM can be realized by loading mixtures of one-component heavy fermionic particles and two-component light fermionic particles into an optical lattice. In a deep enough lattice, the hopping rate of the heavy particles is much lower than the one of the light particles, and it can be ignored. In the model in Eq. (1), we also neglect the trapping potentials. They must be included when realistic MIT is observed and compared with the theoretical calculations.

We study the three-component FKM by using the DMFT. Within the DMFT, the self-energy is a local function of frequency. The Green function of the two-component particles reads

$$G(\mathbf{k}, i\omega_n) = \frac{1}{i\omega_n + \mu - \varepsilon_{\mathbf{k}} - \Sigma(i\omega_n)}, \quad (2)$$

where ω_n is the Matsubara frequency, $\varepsilon_{\mathbf{k}}$ is the dispersion of the two-component particles, and $\Sigma(i\omega_n)$ is the self-energy. Here, we are interested in the homogeneous phase for all particle components, hence the σ index as well as the site index of the self-energy are omitted. The self-energy is determined from the dynamics of a single two-component particle embedded in

an effective self-consistent medium. The action of the effective system reads

$$\begin{aligned}\mathcal{S}_{\rm imp} = &-\int_0^\beta\int_0^\beta d\tau d\tau' \sum_\sigma c_\sigma^\dagger(\tau)\mathcal{G}^{-1}(\tau-\tau')c_\sigma(\tau') \\ &+U_{cc}\int_0^\beta d\tau(c_\uparrow^\dagger c_\uparrow c_\downarrow^\dagger c_\downarrow)(\tau) \\ &+(E_f-\mu)\int_0^\beta d\tau f^\dagger(\tau)f(\tau) \\ &+U_{cf}\int_0^\beta d\tau\sum_\sigma(c_\sigma^\dagger c_\sigma f^\dagger f)(\tau), \end{aligned} \tag{3}$$

where $\mathcal{G}(\tau)$ is a Green function which represents the effective medium. It relates to the self-energy and the local Green function by the Dyson equation

$$\mathcal{G}^{-1}(i\omega_n) = G^{-1}(i\omega_n) + \Sigma(i\omega_n). \tag{4}$$

Here, the local Green function is

$$G(i\omega_n) = \int d\varepsilon\rho_0(\varepsilon)\frac{1}{i\omega_n+\mu-\Sigma(i\omega_n)-\varepsilon}, \tag{5}$$

where $\rho_0(\varepsilon) = \sum_{\mathbf{k}}\delta(\varepsilon-\varepsilon_{\mathbf{k}})$ is the bare density of states (DOS). Without loss of generality, we use the semicircular DOS

$$\rho_0(\varepsilon) = \frac{2}{\pi D^2}\sqrt{D^2-\varepsilon^2}, \tag{6}$$

where D is the half bandwidth. We will use D as the unit of energy. With the semicircular DOS, from Eqs. (4) and (5), we obtain[24]

$$\mathcal{G}^{-1}(i\omega_n) = i\omega_n+\mu-\frac{D^2}{4}G(i\omega_n). \tag{7}$$

One can notice that the occupation number of localized particles in the effective action in Eq. (3) is conserved. It can take only two values: 0 and 1. Therefore the partition function of the effective action can be evaluated independently in the sectors of $f^\dagger f = 0,1$. We obtain

$$\begin{aligned}\mathcal{Z}_{\rm imp} &= {\rm Tr}_f\int\prod_\sigma \mathcal{D}c_\sigma^\dagger\mathcal{D}c_\sigma e^{-\mathcal{S}_{\rm imp}} \\ &= \int\prod_\sigma \mathcal{D}c_\sigma^\dagger\mathcal{D}c_\sigma e^{-\mathcal{S}_0[c_\sigma^\dagger,c_\sigma]} \\ &\quad + e^{-\beta(E_f-\mu)}\int\prod_\sigma \mathcal{D}c_\sigma^\dagger\mathcal{D}c_\sigma e^{-\mathcal{S}_1[c_\sigma^\dagger,c_\sigma]} \\ &= \mathcal{Z}_0 + e^{-\beta(E_f-\mu)}\mathcal{Z}_1, \end{aligned} \tag{8}$$

where

$$\mathcal{Z}_m = \int\prod_\sigma \mathcal{D}c_\sigma^\dagger\mathcal{D}c_\sigma e^{-\mathcal{S}_m[c_\sigma^\dagger,c_\sigma]}, \tag{9}$$

$$\begin{aligned}\mathcal{S}_m[c_\sigma^\dagger,c_\sigma] = &-\int_0^\beta\int_0^\beta d\tau d\tau'\sum_\sigma c_\sigma^\dagger(\tau)[\mathcal{G}^{-1}(\tau-\tau') \\ &-mU_{cf}\delta(\tau-\tau')]c_\sigma(\tau') \\ &+U_{cc}\int_0^\beta d\tau(c_\uparrow^\dagger c_\uparrow c_\downarrow^\dagger c_\downarrow)(\tau), \end{aligned} \tag{10}$$

with $m = 0,1$. In contrast to the spinless case of the FKM,[18,25] the partition function in Eq. (9) cannot be evaluated analytically. It has the same form of the partition function of a single site of the Hubbard model embedded in an effective mean-field medium.[24] Suppose we can solve the effective action in Eq. (10) and obtain the Green function

$$\begin{aligned}G_m(i\omega_n) &= -\frac{\delta\ln\mathcal{Z}_m}{\delta\lambda(i\omega_n)} \\ &= \frac{1}{i\omega_n+\mu-\lambda(i\omega_n)-mU_{cf}-\Sigma_m(i\omega_n)}, \end{aligned} \tag{11}$$

where $\lambda(i\omega_n) = i\omega_n+\mu-\mathcal{G}^{-1}(i\omega_n)$, and $\Sigma_m(i\omega_n)$ is the corresponding self-energy due to the local Coulomb interaction U_{cc}. Once the self-energy $\Sigma_m(i\omega_n)$ is known, the Green function of the effective action in Eq. (3) can also be determined. We obtain

$$\begin{aligned}G_{\rm imp}(i\omega_n) &= -\frac{\delta\ln\mathcal{Z}_{\rm imp}}{\delta\lambda(i\omega_n)} \\ &= \frac{w_0}{i\omega_n+\mu-\lambda(i\omega_n)-\Sigma_0(i\omega_n)} \\ &\quad + \frac{w_1}{i\omega_n+\mu-\lambda(i\omega_n)-U_{cf}-\Sigma_1(i\omega_n)}, \end{aligned} \tag{12}$$

where

$$w_m = \frac{e^{-m\beta(E_f-\mu)}\mathcal{Z}_m}{\mathcal{Z}_{\rm imp}}. \tag{13}$$

One can notice that $w_0+w_1 = 1$, and w_1 is just the filling of localized particles. Basically, the Green function of the effective action in Eq. (12) has the same structure of the one of the spinless case,[18,25] except of the additional self-energy $\Sigma_m(i\omega_n)$ due to the local Coulomb interaction between the hopping particles. The self-consistent condition of the DMFT requires that the Green function obtained from the effective action in Eq. (3) must coincide with the local Green function in Eq. (5), i.e.,

$$G_{\rm imp}(i\omega_n) = G(i\omega_n). \tag{14}$$

Now we obtain the complete self-consistent system of equations for the Green function. It can be solved numerically by iterations.[24] The most time consuming part is the solving of the action $\mathcal{S}_m$ in Eq. (10). We apply ED to solve it.[24,27] The action in Eq. (10) describes the dynamics of an impurity with the repulsive interaction coupling with a conduction bath. It is essentially equivalent to the Anderson impurity model

$$\begin{aligned}H_m = &(\mu-mU_{cf})\sum_\sigma c_\sigma^\dagger c_\sigma + U_{cc}c_\uparrow^\dagger c_\uparrow c_\downarrow^\dagger c_\downarrow \\ &+\sum_{p,\sigma}V_p a_{p\sigma}^\dagger c_\sigma + {\rm H.c.} + \sum_{p,\sigma}E_p a_{p\sigma}^\dagger a_{p\sigma}, \end{aligned} \tag{15}$$

where $a_{p\sigma}^\dagger$ ($a_{p\sigma}$) is the creation (annihilation) operator, which represents the conduction bath with the energy level E_p. V_p is the coupling of the conduction bath with the impurity. The connection between the Anderson impurity model in Eq. (15) and the action in Eq. (10) is the following identity relation of

the bath parameters:[24,27]

$$\sum_p \frac{V_p^2}{i\omega_n - E_p} = \lambda(i\omega_n). \tag{16}$$

To carry out the ED, the conduction bath is limited to finite n_s orbits ($p = 1,2,...,n_s$). Then the bath Green function $\mathcal{G}^{-1}(i\omega_n)$ is approximated by

$$\mathcal{G}_{n_s}^{-1}(i\omega_n) = i\omega_n + \mu - mU_{cf} - \lambda_{n_s}(i\omega_n), \tag{17}$$

where $\lambda_{n_s}(i\omega_n) = \sum_{p=1}^{n_s} V_p^2/(i\omega_n - E_p)$. The bath parameters are determined from minimization of the distance d between $\mathcal{G}^{-1}(i\omega_n)$ and $\mathcal{G}_{n_s}^{-1}(i\omega_n)$:

$$d = \frac{1}{M+1}\sum_{n=0}^{M} \omega_n^{-k} \left|\mathcal{G}^{-1}(i\omega_n) - \mathcal{G}_{n_s}^{-1}(i\omega_n)\right|^2, \tag{18}$$

where M is a large upper cutoff of the Matsubara frequencies.[24,27] The parameter k is introduced to enhance the importance of low Matsubara frequencies in the minimization procedure. In particular, we take $k = 1$ in the numerical calculations. We use the LISA package to find the bath parameters as well as to perform the ED.[24] When the bath parameters are determined, we calculate the Green function of the Anderson impurity model in Eq. (15) by ED.[24,27] In particular, the numerical results presented in the following sections are obtained by ED with the bath size $n_s = 4$. For the single-band Hubbard model, the bath size $n_s = 4$ already gives good quantitative results at low temperature in comparison with the Monte Carlo simulations.[24] We have also checked some numerical results by comparing them with the ones calculated with the bath size $n_s = 5$. A careful analysis of the ED DMFT shows that two bath levels per impurity orbit usually give adequate results.[28] When the ED is performed, we compute the Green function and its self-energy at temperature $T = 0.01$. We consider the grand canonical ensemble and take the filling of localized particles n_f as an input parameter, instead of the energy level E_f. As we have noticed $w_1 = n_f$ that simplifies the numerical calculations.

III. METAL-INSULATOR TRANSITIONS

A. General filling case

As we have mentioned in the previous section, the three-component FKM has two well-known limiting cases. When $U_{cf} = 0$, the Hamiltonian of the hopping particles is just the single-band Hubbard model. At half-filling an MIT occurs at low temperature and this transition is of first order. There is a finite range of the Coulomb interaction $U_{c1} < U_{cc} < U_{c2}$, where both metallic and insulating phases coexist.[21,24] When $U_{cc} = 0$, the three-component FKM is equivalent to the spinless one. For the homogeneous phase, an MIT also occurs at half-filling. In contrast to the single-band Hubbard model, this transition is continuous at the transition point $U_{cf}^c = D$.[18] The situation may completely change when both U_{cc} and U_{cf} terms take effect. First, we summarize the particle filling conditions at which an MIT can occur. In Fig. 1, we plot the particle filling diagram for MIT. The lines in this figure show the filling values of n and n_f at which the

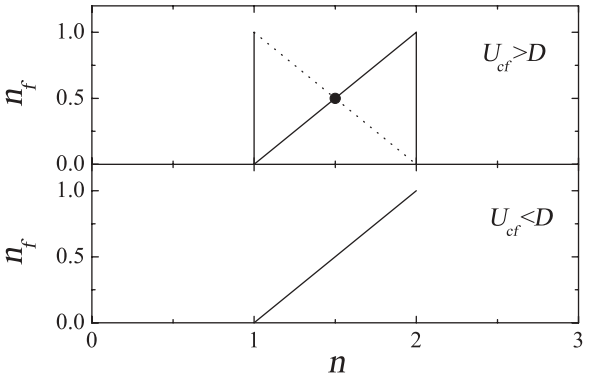

FIG. 1. Diagram of particle fillings for the MIT. The solid lines show the filling values of (n,n_f) at which the MIT can occur, and the dotted line shows the filling values of (n,n_f) for the occurrence of the inverse MIT. The black point indicates the filling value ($n = 3/2, n_f = 1/2$) for the reentrant effect of the MIT.

MIT can occur. Outside these lines no MIT is observed. There is also a possibility of the transition from insulator to metal when the driven interaction increases. We refer the transition as an inverse MIT. In Fig. 1, the particle filling condition for the inverse MIT is presented by the dotted line. The particle filling diagram is different when $U_{cf} > D$ and $U_{cf} < D$ as shown in Fig. 1. In the homogeneous phase, $n = 2n_{c\sigma} + n_f$. The MIT can occur when $1 < n < 2$. In this case, always $n_{c\sigma} = 1/2$ independently whether $U_{cf} > D$ or $U_{cf} < D$. Therefore the MIT is driven only by U_{cc} like in the single-band Hubbard model. The MIT can occur only at $n_{c\sigma} = 1/2$ where every lattice site is occupied by one light particle and their strong local Coulomb interaction does not allow the double occupation of the light particles. The MIT may be interpreted as a species selective MIT, where the two-component light particles are localized due to their Coulomb interaction. The number of heavy particles as well as their Coulomb interaction with the light particles are irrelevant to this MIT. One may also expect that this MIT is of first order. In Fig. 1 one can also see that the MIT can also occur at $n = 1$ or $n = 2$ for $U_{cf} > D$. In this case, the fillings of two-component and one-component particles can be arbitrary, but their total filling is always one-third or two-thirds. The total filling is commensurate with the number of particle components. At $n = 1$, every lattice site is occupied by one particle of any component. The Coulomb interactions (both U_{cc} and U_{cf}) suppress any double occupation of particles. At $n = 2$, the same scenario happens, but with holes instead of particles in the case $n = 1$. We refer this MIT as a commensurate MIT. The same MIT occurs in the three-component Hubbard model.[7,8] In the commensurate MIT, the light and heavy particles play equal roles. The Coulomb interactions prevent any double occupation of particles. In addition to the species selective and commensurate MIT, we also observe the inverse MIT. The inverse MIT can occur when $n_{c\sigma} + n_f = 1$ and $U_{cf} > D$. These conditions are similar to the ones in the spinless FKM.[18] In this case, every lattice site is occupied by one light or one heavy particle. The Coulomb interaction between the light and heavy particles does not allow them to occupy the same lattice site. Since when $U_{cc} = 0$ the system is in the insulating

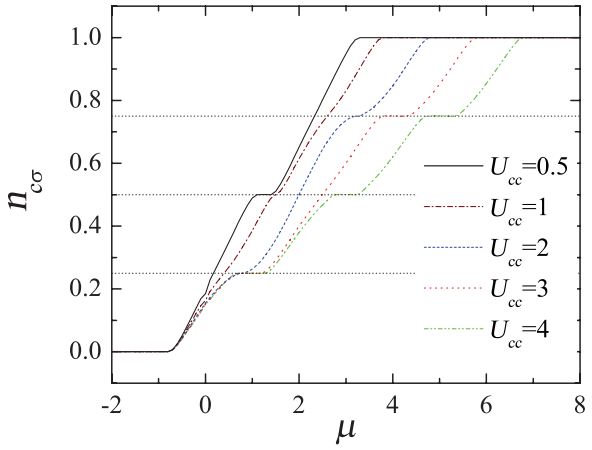

FIG. 2. (Color online) The hopping particle filling $n_{c\sigma}$ as a function of the chemical potential μ at $n_f = 1/2$ for different values of U_{cc} and fixed $U_{cf} = 2$. The horizontal dotted lines show $n_{c\sigma} = 1/4$, $n_{c\sigma} = 1/2$, and $n_{c\sigma} = 3/4$ ($T = 0.01$, $D = 1$).

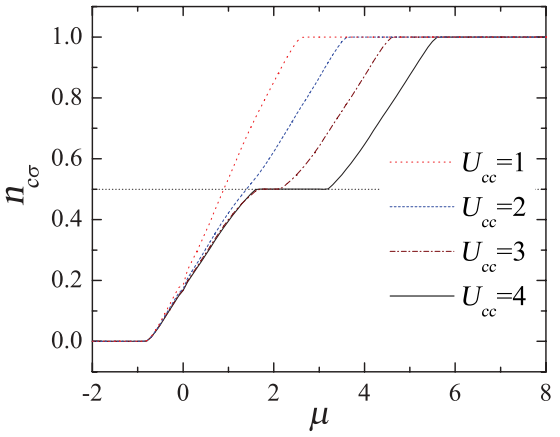

FIG. 3. (Color online) The hopping particle filling $n_{c\sigma}$ as a function of the chemical potential μ at $n_f = 1/2$ for different values of U_{cc} and fixed $U_{cf} = 0.8$. The horizontal dotted line shows $n_{c\sigma} = 1/2$ ($T = 0.01$, $D = 1$).

phase, one may expect that with increasing U_{cc} the system will transform to the metallic phase. When both the MIT and the inverse MIT occur, a reentrant effect of MIT could occur. It happens at half-filling $n = 3/2$ and $n_f = 1/2$.

Next, we present the numerical results to verify the diagram plotted in Fig. 1. For this purpose, we study the dependence of the filling of light particles $n_{c\sigma}$ on the chemical potential μ at a given value of n_f. In the insulating phase when the chemical potential lies in the band gap, the filling $n_{c\sigma}$ does not change. The graphics of the filling $n_{c\sigma}$ as a function of the chemical potential must show a plateau when the chemical potential lies in the band gap. In Fig. 2, we present the numerical results of $n_{c\sigma}$, which are obtained by solving the self-consistent equations of the DMFT plus ED, as a function of the chemical potential at $n_f = 1/2$ and $U_{cf} = 2$. Since $U_{cf} > D$, it is clear that for small values of U_{cc} the system is insulating at $n_{c\sigma} = 1/2$. In this insulating phase each lattice site is occupied by one light or one heavy particle, and the Coulomb interaction between them prevent their double occupation. In Fig. 2, it is shown by the plateau of the line with $U_{cc} = 0.5$. With increasing U_{cc} the system changes to a metallic phase, where the graphics of $n_{c\sigma}$ does not exhibit any plateau. It is the inverse MIT, which occurs when $n_{c\sigma} + n_f = 1$. With further increasing U_{cc}, the graphics of $n_{c\sigma}$ begins to develop two plateaus at $n_{c\sigma} = 1/4$ and $3/4$, which correspond to the total filling $n = 1$ and 2. These plateaus signal the insulating phase at one-third and two-thirds of the total filling. The corresponding MIT is commensurate. For sufficient large U_{cc}, an additional plateau appears at $n_{c\sigma} = 1/2$ that indicates the insulating phase at $n_{c\sigma} = 1/2$. Therefore, at $n_{c\sigma} = 1/2$, there is a reentrance of the insulating phase. However, in contrast to the insulating phase at small values U_{cc}, in this insulating phase, each lattice site is occupied by one light particle and the Coulomb interaction of the light particles prevents the double occupation of the light particles, because the same MIT also occurs at small U_{cf}. This species selective MIT does not depend on U_{cf} as well as the number of heavy particles.

In Fig. 3, we plot the filling $n_{c\sigma}$ at $U_{cf} = 0.8$ and $n_f = 1/2$. In this case $U_{cf} < D$, thus the system is metallic when $U_{cc} = 0$. Weak correlations of light particles cannot drive the system out the metallic state. However, with further increasing U_{cc}, the particle correlations drive the system into insulating state. It is shown in Fig. 3, by the appearance of plateau in the graphics of $n_{c\sigma}$. The MIT occurs at $n_{c\sigma} = 1/2$, and it is the species selective MIT. For $U_{cf} < D$, we do not observe any MIT at one-third or two-thirds of the total filling. The correlations between the light and heavy particles is not strong enough to prevent them to occupy the same site. Consequently, the commensurate MIT cannot be established.

We have checked these by analyzing results for both the cases $U_{cf} > D$ and $U_{cf} < D$ at general filling $n_f = p/q$, where p,q are integer ($p < q$). In summary, the three-component FKM exhibits different MIT depending on the particle fillings and the Coulomb interactions. The MIT can be species selective, commensurate or inverse transitions. The species selective MIT occurs at $n_{c\sigma} = 1/2$, while the commensurate MIT occurs only at one-third or two-thirds of total filling. The inverse MIT can occur at $n_{c\sigma} + n_f = 1$ and $U_{cf} > D$. These MIT could be observed by loading mixtures of light and heavy fermionic atoms into an optical lattice with sufficient lattice depth. By measuring the double occupations among the light particles, between the light and heavy particles, one could detect these MIT.

The half and one-third fillings are two special cases of the MIT. In the next two sections, we will study all cases in detail. We will analyze the MIT through the self-energy and the DOS of the light particles. The experimental observations of spectra of the light particles in optical lattices are challenging.

B. Half-filling case

In this section, we study the MIT at half-filling in detail. One can see in Fig. 1 that at half-filling ($n = 3/2$), the MIT can occur only for $n_{c\sigma} = n_f = 1/2$. It turns out that $\mu = (U_{cc} + U_{cf})/2$ with the particle-hole symmetry. In Fig. 4, we present the numerical results of the self-energy $\mathrm{Im}\Sigma(i\omega_n)$ of the light particles for different values of U_{cc} and a fixed U_{cf}. The behavior of $\mathrm{Im}\Sigma(i\omega_n)$ at low frequencies indicates the

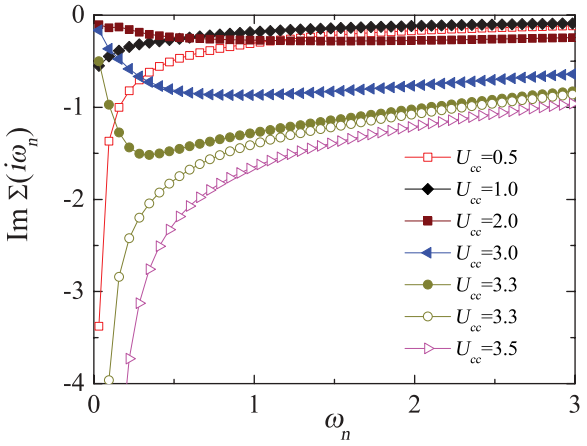

FIG. 4. (Color online) The imaginary part of the light particle self-energy at half-filling for different values of U_{cc} and fixed $U_{cf} = 1.6$. ($T = 0.01$, $D = 1$).

conduction properties of the system. When $\mathrm{Im}\Sigma(i\omega_n)$ diverges as $\omega_n \to 0$, the system is insulating, while when $\mathrm{Im}\Sigma(i\omega_n) \to 0$ as $\omega_n \to 0$, the system is metallic. If $\lim_{\omega_n \to 0} \mathrm{Im}\Sigma(i\omega_n)$ is finite, the system is still metallic, but it does not obey the Fermi liquid properties. Since in Fig. 4, $U_{cf} > D$, one may expect that the system is insulating for small values of U_{cc}. Indeed, in Fig. 4, we can see that $\mathrm{Im}\Sigma(i\omega_n)$ diverges as $\omega_n \to 0$ for $U_{cc} = 0.5$, which indicates the insulating state of the system. With increasing U_{cc}, $\mathrm{Im}\Sigma(i\omega_n)$ stops to diverge as $\omega_n \to 0$. It shows that the system becomes metallic. However, $\mathrm{Im}\Sigma(i\omega_n)$ may tend to a finite value when $\omega_n \to 0$. In Fig. 4, this behavior is shown by the self-energy with $U_{cc} = 1$ and 2. In this regime, the finite value of $\mathrm{Im}\Sigma(i\omega_n)$ when $\omega_n \to 0$ becomes smaller with increasing U_{cc}. With further increasing U_{cc}, $\mathrm{Im}\Sigma(i\omega_n)$ has a tendency of decreasing its value at $\omega_n \to 0$ to zero. This behavior reminisces the Fermi liquid properties. It is shown in Fig. 4 by the self-energy with $U_{cc} = 3$. With further increasing U_{cc}, $\mathrm{Im}\Sigma(i\omega_n)$ diverges as $\omega_n \to 0$, and the system falls into the insulating phase regime again. However, between the metallic and insulating phases, we detect a finite region, where both the metallic and insulating solutions coexist. This feature is similar to the MIT in the single-band Hubbard model.[21,24] In Fig. 4, we present both metallic and insulating self-energies in this region ($U_{cc} = 3.3$). In the coexistent region, distinct metallic and insulating phases do not exist. It is similar to the critical point of classical gases, above which no phase boundaries between vapor and liquid phases exist. From the behaviors of the self-energy, we observe the reentrance of the insulating phase in the region of $U_{cf} > D$. With increasing U_{cc} from zero value, the system first stays in the insulating phase, then the Coulomb interactions drive it into the metallic phase, and finally, the system goes back to the insulating phase. The later MIT is first order, and it crosses a finite region where both the metallic and insulating phases coexist.

The above analyzed phase transitions can also be seen from the behavior of the DOS of the light particles. In Fig. 5, we plot the DOS $\rho(\omega) = -\mathrm{Im}G(\omega + i\eta)/\pi$ for different values of U_{cc} and fixed U_{cf}. In ED we can compute the Green function for both Matsubara and real frequencies. In the numerical calculations, we take $\eta = 0.01$ for broadening the width of

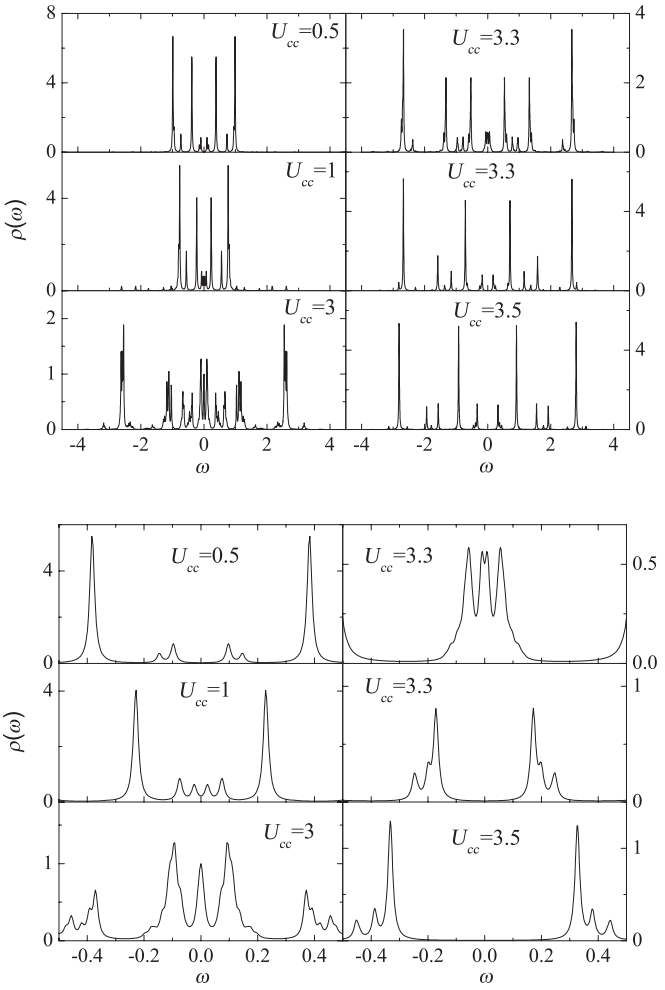

FIG. 5. The DOS of the light particles at half-filling for different values of U_{cc} and $U_{cf} = 1.6$. (Top) DOS at the full energy scale. (Bottom) DOS is focused at low energies. ($T = 0.01$, $D = 1$).

the δ functions. When the DOS shows a gap at the position of the chemical potential ($\omega = 0$), the system is insulating. If the DOS is finite at $\omega = 0$ the system is metallic. Figure 5 shows an MIT between $0.5 < U_{cc} < 1$ at $U_{cf} = 1.6$. For small values of U_{cc}, the DOS exhibits a gap at the Fermi energy. With increasing U_{cc} the gap becomes smaller, and it disappears at the transition point U_c. When $U_{cc} > U_c$, the DOS exhibits a pseudogap at $\omega = 0$. The pseudogap is developed from the gap of the insulating phase. In Fig. 5, this behavior is shown by the DOS with $U_{cc} = 1$. The phase with pseudogap corresponds to the case of finite value of the imaginary part of the self-energy at zero energy. With further increasing U_{cc}, the DOS exhibits a group of narrow peaks around $\omega = 0$. In Fig. 5, it is shown by the DOS with $U_{cc} = 3$. In the single-band Hubbard model, the group of narrow peaks at $\omega = 0$ represents the Kondo resonance.[24,27] However, due to the finite size effect and the discreteness of the ED, the Kondo resonance does not appear at the full scale. Nevertheless, the appearance of the group of narrow peaks at $\omega = 0$ can be interpreted as a signal of the Kondo resonance. However, in contrast to the single-band Hubbard model, the local Green function here is a superposition of two local subband Green functions $G_m(\omega)$ as

one can see from Eq. (12). Each local subband Green function is described by an Anderson impurity with the Coulomb interaction U_{cc} embedded in a conduction bath. The energy level of the Anderson impurity is $\mu - mU_{cf} = (U_{cc} \pm U_{cf})/2$. The Anderson impurity is symmetric when its energy level is placed at $U_{cc}/2$.[29,30] Since $U_{cf} > 0$, the Anderson impurity is asymmetric. Therefore the Kondo resonance that appears in the local subband DOS, must be shifted from the Fermi level.[29,30] Only for the symmetric Anderson impurity, the Kondo resonance peaks at the Fermi level. Consequently, the group of narrow peaks at $\omega = 0$ represents the superposition of the two shifted Kondo peaks. It can be considered as an asymmetric Kondo splitting. Experimental observations of the asymmetric Kondo splitting in the spectra of the light particles are challenging. With tunable value of U_{cf}, experiments could observe the asymmetric Kondo splitting in the spectra of light particles and the splitting width increases with increasing U_{cf}. At U_{c2}, the group of narrow peaks disappears, and the system becomes insulating. However, as in the single-band Hubbard model, the insulating solution exists until $U_{c1} < U_{c2}$. In the region $U_{c1} < U_{cc} < U_{c2}$, both metallic and insulating solutions coexist. Thus the second MIT is of first order. This MIT solely deals with the light particles, because it exists even when U_{cf} is small. The transition is the species selective MIT. In the insulating phase, each lattice site is occupied by one light particle, and the Coulomb interaction prevents the double occupation of the light particles. Experiments could detect the existence of the coexistent region by measuring the double occupation of the light particles. Across the region, the double occupation must exhibit a jump in its value. The MIT mechanisms of the two MITs are different. In the first, inverse MIT, the pseudogap of the metallic phase is developed from the gap of the insulating phase, whereas in the second, species selective MIT, the phase transition occurs due to the collapse of the asymmetric Kondo splitting.

We have also analyzed the MIT through the self-energy and the DOS for the case $U_{cf} < D$. In this case, the MIT is species selective and has the same features as the one in the case $U_{cf} > D$, which we have discussed above. We summarize the phase transitions in the phase diagram plotted in Fig. 6. In the region $U_{cf} > D$, there are two MITs. One is inverse MIT and the other is species selective MIT. At the first transition (U_c), particle correlations drive the system from an insulating to a metallic phase, while at the second one, particle correlations drive the system from a metallic to an insulating phase. A finite region of coexistence of the metallic and insulating phases exists between the species selective MIT. The critical value U_c of the inverse MIT increases with U_{cf}. It vanishes at $U_{cf} = D$. Hence, in the region $U_{cf} < D$, the reentrant effect of the insulating phase is absent. The phase diagram is consistent with the analysis of the phase transitions observed from dependence of $n_{c\sigma}$ on the chemical potential, which have been presented in the previous section.

C. Third-filling case

In this section, we study the MIT at third-filling $n_{c\sigma} = n_f = 1/3$. The MIT is quite different in comparison with the half-filling case. It works with both the light and heavy particles. In numerical calculations, the chemical potential is adjusted in order to maintain $n_{c\sigma} = 1/3$. The two-thirds filling case $n_{c\sigma} = n_f = 2/3$ is the particle-hole symmetry of this one-third filling case. We plot the phase diagram for the third-filling case in Fig. 7. The value U_c at the MIT point quickly increases as U_{cf} approaches to the value D, while it slowly decreases as U_{cf} increases. The insulating phase is established only for sufficient large Coulomb interactions (both U_{cc} and U_{cf}). In the insulating phase, each lattice site is occupied by one particle of the light or heavy particle components, and the Coulomb interactions prevent any double occupation. The MIT can also be analyzed through the self-energy and the DOS of the light particles, as in the case of half-filling. The behaviors of the self-energy in the metallic and insulating phases exhibit similar features as in the half-filling case. However, the features of the DOS are different. In Fig. 8, we plot the DOS for different values of U_{cc} and fixed U_{cf}. One can see from Eq. (12) that the local Green function is a superposition of two subband Green functions with nonequal weights. The Kondo peak, which appears in the local subband DOS, is away from the Fermi energy and is reduced.[29,30] Therefore the peak that appears at the Fermi level in the metallic phase is merely

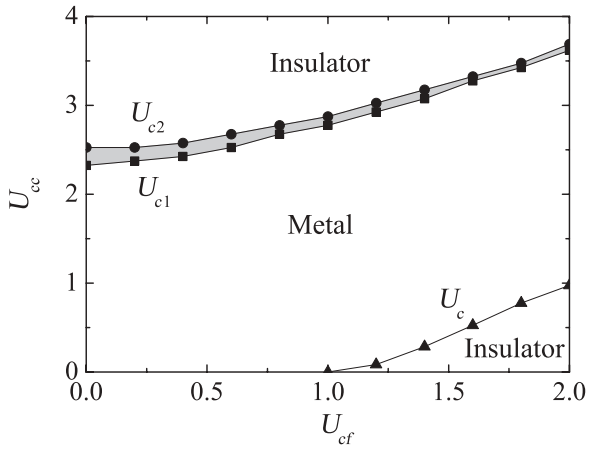

FIG. 6. Phase diagram at half-filling $n_{c\sigma} = n_f = 1/2$. In the grey area, both metallic and insulating phases coexist.

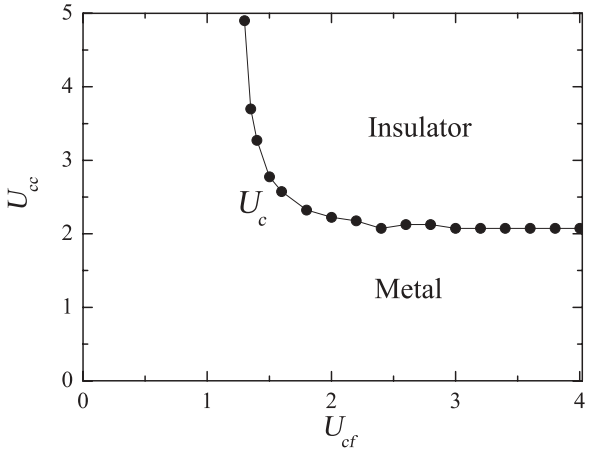

FIG. 7. Phase diagram for third-filling $n_{c\sigma} = n_f = 1/3$. ($T = 0.01$, $D = 1$).

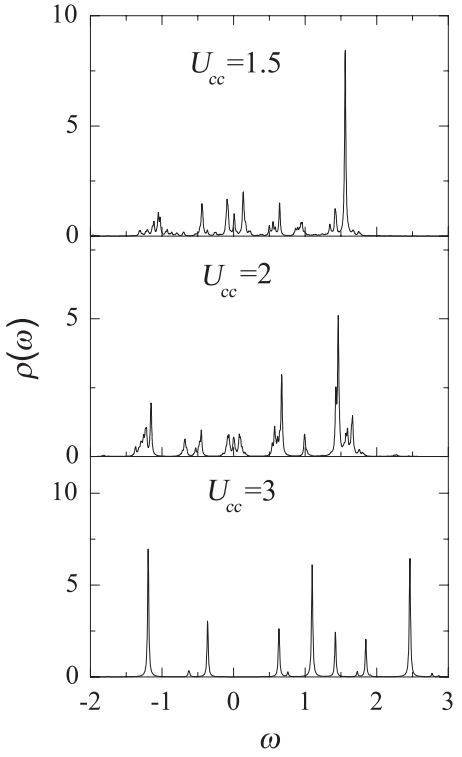

FIG. 8. The DOS of the light particles at third-filling for different values of U_{cc} and fixed $U_{cf} = 2$. ($T = 0.01$, $D = 1$).

the superposition of two local subband DOS, and maybe it is irrelevant to the Kondo resonance. Thus the MIT can occur at the third-filling in contrast to the single-band Hubbard model, where no MIT is observed at third-filling. In contrast to the half-filling case, we do not observe any region of coexistence of metallic and insulating phase. However, close to the MIT, we observe a phase separation that happens at fillings very close to the third-filling. In Fig. 9, we plot the hopping particle filling $n_{c\sigma}$ as a function of the chemical potential μ for various

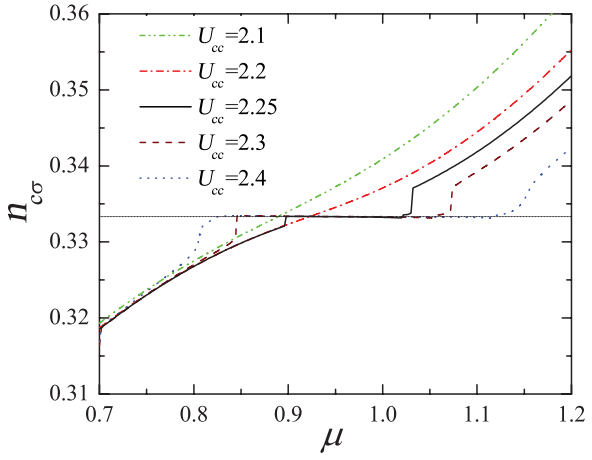

FIG. 9. (Color online) The hopping particle filling $n_{c\sigma}$ as a function of the chemical potential μ for various values of U_{cc} close to the transition value U_c and fixed $U_{cf} = 2$. The horizontal dotted line shows $n_{c\sigma} = 1/3$. ($T = 0.01$, $D = 1$).

values of U_{cc} close to the phase transition point U_c. One can see in Fig. 9, when $U_{cc} < U_c$, the graphics of $n_{c\sigma}$ does not show any plateau at $n_{c\sigma} = 1/3$, which indicates the metallic phase. However, for U_{cc} close to U_c in the insulator side, the graphics of $n_{c\sigma}$ show not only the plateau, which indicates the insulating state, but also a gap at fillings close to $n_{c\sigma} = 1/3$. Within the gap, the filling $n_{c\sigma}$ is uncertainty. This feature indicates a phase separation at those fillings. The MIT at third-filling is commensurate. It does not distinguish the light particles from the heavy ones. Any double occupation must be vanished at the transition point. The MIT is also observed at third-filling in the three-component Hubbard model.[7,8] One can notice that the commensurate MIT always occurs at the commensurate fillings independently whether the mass imbalance or the interaction anisotropy exist or not. Working at the commensurate fillings, experiments could detect this MIT.

IV. CONCLUSION

We have studied the MIT in the three-component FKM by using the DMFT with ED. We find the conditions for the particle fillings at which the MIT can occur. In particular, the MIT can occur at total filling $1 \leqslant n \leqslant 2$. When the total filling $1 < n < 2$, the MIT is species selective, and it can occur only at half-filling of the light particles ($n_{c\sigma} = 1/2$). At the total filling of one-third or two-thirds, the MIT can occur only at sufficient strong Coulomb interactions. This MIT works with both light and heavy particles. We also observe the inverse MIT, i.e., the phase transition from insulator to metal when the Coulomb interactions increase. The inverse MIT can occur only for sufficient strong correlations between light and heavy particles, and the particle filling condition $n_{c\sigma} + n_f = 1$. We have also studied in detail the MIT at half- and third-filling. At half-filling, the reentrant effect of insulating phase is observed. As the Coulomb interactions increase, the system first stays in the insulating phase, then it becomes metallic, and finally, it goes back to the insulating phase. The first MIT is continuous, while the second one is discontinuous. As in the single-band Hubbard model, we also observe a finite region at the second MIT, where both metallic and insulating phases coexist. However, in contrast to the single-band Hubbard model, the MIT occurs together with asymmetric Kondo splitting in the spectra of the light particles. At the third-filling, the MIT can occur only for sufficient strong Coulomb interactions. We find the phase separation close to MIT point from the insulator side. We have also constructed the phase diagram at half- and third-filling. However, in this paper, we still restrict ourselves to consider only the homogeneous phases. At low temperature, one may expect the stability of charge- (or/and spin-) density-wave states. We leave these phases for further studies.

ACKNOWLEDGMENTS

This research is funded by Vietnam National Foundation for Science and Technology Development (NAFOSTED) under grant No. 103.02-2011.29.

[1]N. F. Mott, *Metal insulator transitions* (Taylor and Francis, London, 1990).
[2]I. Bloch, J. Dalibard, and W. Zwerger, Rev. Mod. Phys. **80**, 885 (2008).
[3]R. Jördens, N. Strohmaier, K. Günter, H. Moritz, and T. Esslinger, Nature (London) **455**, 204 (2008).
[4]U. Schneider, L. Hackermüller, S. Will, Th. Best, I. Bloch, T. A. Costi, R. W. Helmes, D. Rasch, and A. Rosch, Science **322**, 1520 (2008).
[5]F. M. Spiegelhalder, A. Trenkwalder, D. Naik, G. Hendl, F. Schreck, and R. Grimm, Phys. Rev. Lett. **103**, 223203 (2009).
[6]S. Taie, Y. Takasu, S. Sugawa, R. Yamazaki, T. Tsujimoto, R. Murakami, and Y. Takahashi, Phys. Rev. Lett. **105**, 190401 (2010).
[7]E. V. Gorelik and N. Blümer, Phys. Rev. A **80**, 051602(R) (2009).
[8]K. Inaba, S. Y. Miyatake, and S. I. Suga, Phys. Rev. A **82**, 051602(R) (2010).
[9]T.-L. Dao, M. Ferrero, P. S. Cornaglia, and M. Capone, Phys. Rev. A **85**, 013606 (2012).
[10]J. K. Freericks, M. M. Maska, A. Hu, T. M. Hanna, C. J. Williams, P. S. Julienne, and R. Lemanski, Phys. Rev. A **81**, 011605 (2010); **82**, 039901(E) (2010).
[11]C. Ates and K. Ziegler, Phys. Rev. A **71**, 063610 (2005).
[12]L. M. Falicov and J. C. Kimball, Phys. Rev. Lett. **22**, 997 (1969).
[13]T. Kennedy, Rev. Math. Phys. **6**, 901 (1994).
[14]T. Portengen, Th. Östreich, and L. J. Sham, Phys. Rev. B **54**, 17452 (1996).
[15]Tran Minh-Tien, Phys. Rev. B **67**, 144404 (2003).
[16]V.-N. Phan and M.-T. Tran, Phys. Rev. B **72**, 214418 (2005).
[17]U. Brandt, A. Fledderjohann, and G. Hülsenbeck, Z. Phys. B **81**, 409 (1990).
[18]J. K. Freericks and V. Zlatic, Rev. Mod. Phys. **75**, 1333 (2003).
[19]J. Jedrzejewski and V. Derzhko, Physica A **317**, 227 (2003).
[20]J. Hubbard, Proc. R. Soc. London A **281**, 401 (1964).
[21]A. Georges and G. Kotliar, Phys. Rev. B **45**, 6479 (1992).
[22]M. J. Rozenberg, G. Kotliar, and X. Y. Zhang, Phys. Rev. B **49**, 10181 (1994).
[23]W. Metzner and D. Vollhardt, Phys. Rev. Lett. **62**, 324 (1989).
[24]A. Georges, G. Kotliar, W. Krauth, and M. J. Rozenberg, Rev. Mod. Phys. **68**, 13 (1996).
[25]U. Brandt and C. Mielsch, Z. Phys. B **75**, 365 (1989).
[26]Q. Si, G. Kotliar, and A. Georges, Phys. Rev. B **46**, 1261 (1992).
[27]M. Caffarel and W. Krauth, Phys. Rev. Lett. **72**, 1545 (1994).
[28]A. Liebsch and H. Ishida, J. Phys.: Condens. Matter **24**, 053201 (2012).
[29]A. C. Hewson, *The Kondo Problem to Heavy Fermions* (Cambridge University Press, Cambridge, 1997).
[30]B. Horvatic, D. Sokcevic, and V. Zlatic, Phys. Rev. B **36**, 675 (1987).